

Exploring Finite Temperature Properties of Materials with Quantum Computers

Connor Powers,^{1, 2} Lindsay Bassman,¹ and Wibe A. de Jong¹

¹*Lawrence Berkeley National Lab, Berkeley, CA 94720*

²*University of Maryland, College Park, MD 20742*

Thermal properties of nanomaterials are crucial to not only improving our fundamental understanding of condensed matter systems, but also to developing novel materials for applications spanning research and industry alike. Since quantum effects arise at the nanomaterial scale, these systems are difficult to simulate on classical computers. Quantum computers, by contrast, can efficiently simulate quantum many-body systems. However, current algorithms for calculating thermal properties of these systems incur significant computational costs in that they either prepare the full thermal (i.e., mixed) state on the quantum computer, or else they must sample a number of pure states from a distribution that grows with system size. Canonical thermal pure quantum states provide a promising path to estimating thermal properties of quantum materials as they neither require preparation of the full thermal state nor require a large number of samples. Remarkably, fewer samples are required as the system size grows. Here, we present a method for preparing canonical TPQ states on quantum computers and demonstrate its efficacy in estimating thermal properties of quantum materials. Due to its increasing accuracy with system size, as well as its flexibility in implementation, we anticipate that this method will enable finite temperature explorations of relevant quantum materials on near-term quantum computers.

Introduction- As the search for high-performance materials persists in research and industry alike, there is a need for better understanding the thermal properties of materials. In particular, exploring thermal properties of nanomaterials is of great interest, with applications ranging from energy production to nanoelectronics [1, 2]. However, quantum effects dominate at this scale, which poses a challenge for traditional computational methods. Due to the exponential growth of resources required to simulate quantum many-body systems with classical computers, the exploration of materials at this scale quickly exceeds the capabilities of even the largest classical supercomputers [3]. Quantum computers, by contrast, are able to simulate quantum many-body systems efficiently, potentially providing an advantage over classical computers [4, 5]. Therefore, quantum computers offer a potential route to studying thermal properties of quantum materials. While a plethora of zero-temperature simulations have been demonstrated on quantum devices in recent years [6–9], the landscape of quantum algorithms to calculate finite temperature properties remains more sparse. The main challenge in exploring finite-temperature properties of such systems on quantum computers lies in the preparation of thermal states.

Current algorithms for thermal state preparation fall into two main categories. The first is comprised of algorithms that initialize the qubits into the full thermal (i.e., mixed) state. In this case, the thermal average of an observable can be computed directly by measuring the observable in this state. Examples include algorithms that prepare the Gibbs state using phase estimation [10–12], which require quantum circuits that are too large for near-term quantum devices, otherwise known as noisy intermediate-scale quantum (NISQ) computers [13]. Other examples include the variational quantum thermalizer [14] and methods that prepare thermofield

double states [1, 15], both of which rely on variational techniques. The variational nature of these algorithms necessitates the use of a cost function, which generally becomes hard to compute as system size increases. Such methods are therefore difficult to scale to large or complex systems. Still other methods for generating the full thermal state require a number of ancilla qubits that scales with system size or complexity [16, 17], thus limiting the size of systems that can be simulated on current quantum hardware.

Algorithms in the second category, prepare an ensemble of pure states, one pure state at a time, where each pure state has been sampled according to the correct thermal statistics. Existing examples rely on Monte Carlo sampling techniques, Markov chains, or both [18–23]. To calculate thermal averages, the desired observable is measured in each of the different pure states and the results are averaged over the ensemble. As pure states are much easier to prepare on a quantum computer than mixed states, this model for thermal state preparation is more promising for NISQ computers. However, the number of samples required generally grows with the size of the system being simulated, which can lead to significant resource requirements for large systems.

Canonical thermal pure quantum (TPQ) states [24] offer a promising new way to estimate thermal averages on quantum computers. Thermal state approximation by TPQ states lies in a separate third category, as it neither incurs the quantum resources required to prepare the full thermal state nor relies on sampling techniques like Monte Carlo whose required number of samples tends to increase with system size. TPQ states are formed by applying a specific non-unitary transformation, which is a function of the system Hamiltonian and inverse temperature, to a random state. The resulting state is shown to be representative of the thermal equilibrium in that observables measured in this state will approximate ther-

mal averages. Remarkably, the error in the expectation value of the observable is bounded by an exponentially decreasing function of system size. Thus, at sufficiently large N , the expectation value of an observable in only a single TPQ state will yield a very close approximation to the thermal average. The effectiveness of canonical TPQ states has been demonstrated classically [24], but to our knowledge, has not been implemented on a quantum computer.

Here, we present an algorithm for generating canonical TPQ states on quantum computers with low quantum resource requirements, enabling the estimation of finite temperature properties of materials on NISQ devices. Our algorithm relies on a straightforward and scalable protocol for preparing the random state [25], which allows for circuit depths to be tuned to find a balance between desired accuracy and feasibility of execution on NISQ hardware. Furthermore, the algorithm is agnostic to implementation of the non-unitary transformation of the random state, which can be tailored to the resource constraints of different quantum devices. We outline two possible implementations for approximating the non-unitary transformation: (i) the quantum imaginary time evolution (QITE) algorithm [18], which is best suited to devices constrained in qubit count, and (ii) the dilated operator approach [26], which is best suited for devices with limited coherence times.

We demonstrate our algorithm using each implementation for the Heisenberg model, a quintessential model used for studying a range of behaviors in materials [27–31]. We anticipate that this algorithm will facilitate estimations of finite temperature properties of materials on near-term quantum devices. Furthermore, since error in estimating thermal averages with TPQ states decreases with increasing system size, we believe this algorithm will only become increasingly useful as quantum hardware continues to grow in size in the coming years.

Theory background and framework- The canonical TPQ state of a system of size N , governed by Hamiltonian H , at inverse temperature β is defined as [24]

$$|\beta, N\rangle = \hat{Q} |\Psi_R\rangle \equiv e^{-\beta H/2} |\Psi_R\rangle \quad (1)$$

where $|\Psi_R\rangle = \sum_{i=1}^{2^N} c_i |i\rangle$ is a random state, where complex amplitudes c_i are uniformly sampled from the unit sphere such that $\sum_{i=1}^{2^N} |c_i|^2 = 1$, and $|i\rangle$ is an arbitrary orthonormal basis. Defined this way, $|\Psi_R\rangle$ is characterized as a Haar-random pure state [32]. We define

$$\langle \hat{A} \rangle_{\beta, N}^{\text{ens}} \equiv \frac{\text{Tr}[e^{-\beta H} \hat{A}]}{\text{Tr}[e^{-\beta H}]} \quad (2)$$

as the ensemble expectation value of an operator \hat{A} for a system of size N at inverse temperature β , and

$$\langle \hat{A} \rangle_{\beta, N}^{\text{TPQ}} \equiv \frac{\langle \beta, N | \hat{A} | \beta, N \rangle}{\langle \beta, N | \beta, N \rangle} \quad (3)$$

as the corresponding expectation value of \hat{A} in a single TPQ state. It is noted that \hat{A} must be a low-degree

polynomial of local operators for the following analysis to hold, but this group contains many prominently used observables including energy, magnetization, and a number of relevant correlation functions. The error between $\langle \hat{A} \rangle_{\beta, N}^{\text{TPQ}}$ and $\langle \hat{A} \rangle_{\beta, N}^{\text{ens}}$ is bounded by a value that becomes exponentially small with increasing system size N [24]. In practice, this means that for sufficiently large N , measuring the desired observable in a single TPQ state will provide a good approximation of the true thermal average. Indeed, Ref. [24] found less than a 1% error when estimating thermal properties using a single TPQ state for a quantum spin model with $N = 30$. At lower N , fidelity can be increased by averaging over the measured values from multiple TPQ states [24].

The first step in preparing these TPQ states on a quantum computer is the preparation of $|\Psi_R\rangle$. We can approximate this Haar-random state using random quantum circuits constructed in the manner proposed in Ref. [25] and illustrated in Fig. 1.

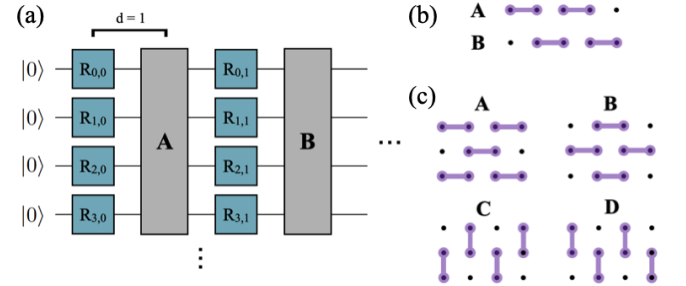


FIG. 1: (a) Gate pattern for approximate Haar-random circuits. $R_{i,j}$ are randomly selected single-qubit rotation gates selected from a finite set with constraints (see main text). In 1D systems 2-qubit layers follow the pattern **ABAB...** with individual layer patterns specified in (b), while in 2D systems, 2-qubit layers follow the pattern **ABCDABCD...**, with individual layer patterns specified in (c).

The random circuits considered in this letter are composed of “blocks,” where each block is composed of a layer of single-qubit rotation gates on every qubit followed by a layer of two-qubit entangling gates. The single-qubit rotation gates are selected from a finite set $\mathbb{A} = \{Rx(\frac{\pi}{2}), Ry(\frac{\pi}{2}), T\}$, with the constraint that no gate may be chosen for the same qubit two blocks in a row. In other words, if $R_{i,j}$ is the j th single-qubit gate acting on qubit i , then $R_{i,j} \in \mathbb{A} \setminus R_{i,j-1}$.

The two-qubit gate layers, as shown in Fig. 1b-c, follow a fixed pattern determined by the dimension of the Hamiltonian of interest; if this dimension is k , there will be $2k$ different two-qubit gate layer patterns to loop through to ensure all coupling directions have been accounted for. In this way, the random circuits are easily generalizable to higher dimensions. For example, Fig. 1b shows the two 2-qubit gate patterns that must be looped through for a 1D system. Similarly, Fig. 1c shows the four

2-qubit gate patterns to loop through for 2D systems.

Random circuits of this form can be defined by a single parameter d , which sets the number of blocks and ultimately controls the circuit depth. Such circuits can be shown to generate states whose properties converge to those of Haar-random states with increasing d . We can see this convergence by plotting the entropy of the resulting random state. This plot is useful for determining how large d needs to be for a given system size; the necessary d will be the point at which the state entropy is sufficiently converged to the value $\ln N - 1 + \gamma$ characteristic of Haar-random states, where $\gamma \approx 0.577$ is the Euler-Mascheroni constant. See the Supplementary Information for details. Here, we set $d = 20$, unless otherwise specified.

Once the random state $|\Psi_R\rangle$ has been generated, it must be evolved under the non-unitary operator \hat{Q} to generate a canonical TPQ state. This can be implemented by any method for approximating non-unitary transformations on quantum computers, and in practice method choice is informed by available quantum resources. Here, we demonstrate our algorithm with two different approaches, including QITE [18] and a dilated operator approach [26]. Using QITE, the overall algorithm requires no ancillary qubits or post-selection, at the cost of deeper circuits that require significant classical resources to construct. Using unitary dilation, the overall algorithm requires post-selection and a single ancillary qubit, yet generates shallower circuits. Algorithm 1 summarizes our method for approximating thermal averages with TPQ states on quantum computers.

Algorithm 1: Pseudocode for computation of thermal averages with canonical TPQ states on quantum computers.

```

Input:  $H, \hat{A}, \beta, R, d, k$ 
Output:  $\langle \hat{A} \rangle_{\beta, N}^{\text{TPQ}} \approx \langle \hat{A} \rangle_{\beta, N}^{\text{ens}}$ 
1 thermal_vals = []
  /* Loop over  $R$  TPQ state realizations */
2 for  $n=[0, R]$  do
  /* make random state preparation circuit */
3   random_circ=empty_circuit()
4   prev_layer=[]
  /* Loop over  $d$  to add  $d$  blocks */
5   for  $j=[0, d]$  do
    /* add single qubit gate layer */
6     single_qub_layer = SingleQubLayer(prev_layer)
7     random_circ.append(single_qub_layer)
8     prev_layer = single_qub_layer
    /* Add two-qubit gate layer */
9     random_circ.append(TwoQubLayer( $k, j$ ))
  /* Approximate transformation under  $\hat{Q}$  */
10    Q_circ = nonunitary_approx_circ( $H, \beta, \dots$ )
11    TPQ_state_circ = random_circ + Q_circ
  /* measure observable of interest */
12    thermal_val = measure(TPQ_state_circ,  $\hat{A}$ )
13    thermal_vals.append(thermal_val)
14 return average(thermal_vals)

```

First, the d -layer circuit is constructed. Layers of randomly chosen single-qubit rotation gates are alternated with layers of 2-qubit entangling gates following a pattern set by Hamiltonian dimension k . Then, the system is evolved under a unitary approximation of the non-unitary transformation under \hat{Q} . The algorithm is flexible in how this non-unitary operation is implemented. The observable of interest is then measured in the resulting canonical TPQ state, and this process is repeated R times to construct and measure R distinct TPQ states. Finally, if applicable, the average of the measured thermal values is taken.

If QITE is chosen to implement line 12 in Algorithm 1, the non-unitary operation is broken up into timesteps of imaginary time evolution, and each timestep is approximated by a unitary circuit. Increasing the number of timesteps increases overall transformation fidelity, yet at a linearly scaling cost of quantum gates. When using QITE, a couple additional parameters are required, including a domain size and an imaginary timestep size.

If line 12 in Algorithm 1 is instead implemented with the dilated operator approach, an ancillary qubit initialized in state $|1\rangle$ must be added to create the supplemented input state $\rho_{in} = (|1\rangle\langle 1|) \otimes \rho_R$, where $\rho_R = |\Psi_R\rangle\langle \Psi_R|$. A dilated unitary operator $\hat{\Omega}$ is then constructed in the new 2^{N+1} dimensional Hilbert space that will approximate the action of \hat{Q} on the original 2^N dimensional system Hilbert space [26]. $\hat{\Omega}$ is defined in terms of the non-unitary operator \hat{Q} as

$$\hat{\Omega} \equiv \exp\left(i\epsilon \begin{pmatrix} 0 & -i\hat{Q} \\ i\hat{Q}^\dagger & 0 \end{pmatrix}\right) \quad (4)$$

where ϵ is a parameter that controls the performance of the operator. The supplemented initial state ρ_{in} is then evolved under the dilated unitary operator $\hat{\Omega}$ and the ancillary qubit is measured. If it is measured in state $|0\rangle$, the N -qubit system of interest has been transformed by the effective operator $U^\dagger \sin(\epsilon\Sigma) V$, where $U^\dagger \Sigma V$ is the singular value decomposition of the desired operator \hat{Q} [26].

To help quantify the performance of this dilated operator, it is useful to define a fidelity metric to indicate how close our effective transformation on the N -qubit system is to the desired non-unitary transformation under \hat{Q} . This fidelity can be defined as:[26]

$$F = \text{Tr} \sqrt{\sqrt{\rho_0} |\beta, N\rangle \langle \beta, N| \sqrt{\rho_0}} \quad (5)$$

Here, ρ_0 is the density matrix of the N -qubit system after tracing out the ancillary qubit, provided that it is measured in state $|0\rangle$. The probability of transformation success P_0 and transformation fidelity F can exhibit complex dependence on ϵ , and this dependence is also affected by the desired non-unitary operator. In the low- ϵ regime that is practical for this transformation, lower ϵ generally yields a higher transformation fidelity and a lower probability of success. See the Supplementary Information

for more on this behavior. While this method introduces a single ancillary qubit, its advantage is that increasing fidelity to the desired non-unitary transformation only entails a larger number of required shots. This stands in contrast to the QITE algorithm, where increasing fidelity for a given domain size requires a larger number of imaginary timesteps and subsequently deeper circuits. If the dilated operator approach is preferred, then the only change in Algorithm 1 is the addition of an ancillary qubit initialized in the $|1\rangle$ state which is not included in the random circuit construction. The non-unitary transformation approximation step then takes in the additional argument ϵ .

Results- We now demonstrate our algorithm by calculating the thermal energy of a Heisenberg spin chain under an external magnetic field at various system sizes and inverse temperatures. The Hamiltonian of an N -spin Heisenberg chain is given by

$$\hat{H} = \sum_{\alpha} \sum_{\langle i,j \rangle} J_{\alpha} \sigma_i^{\alpha} \sigma_j^{\alpha} + h_x \sum_{i=1}^N \sigma_i^x \quad (6)$$

where J_{α} ($\alpha \in \{x, y, z\}$) gives the strength of the exchange coupling interaction between nearest neighbor spin pair $\langle i, j \rangle$ in the α -direction, h_x is the strength of an externally applied magnetic field in the x -direction, and σ^{α} are Pauli matrices. For results presented in this letter, we set $J_x = 0.5$, $J_y = 1.25$, $J_z = 2.0$, and $h_x = 1.0$.

Fig. 2a demonstrates observed error trends with increasing system size N , averaged over results from $R = 100$ distinct TPQ states, for a 1D Heisenberg model at inverse temperature $\beta = 0.5$. The squared error is shown to generally trend down as system size increases, which aligns with expectations from TPQ state formalism. For low N , the error from utilizing a single TPQ state may become large. Fig. 2b demonstrates that averaging over the results from multiple TPQ states can reduce such error. In this example, the observable of interest is the thermal energy as a function of inverse temperature β , and the simulated system is a 6-spin Heisenberg model.

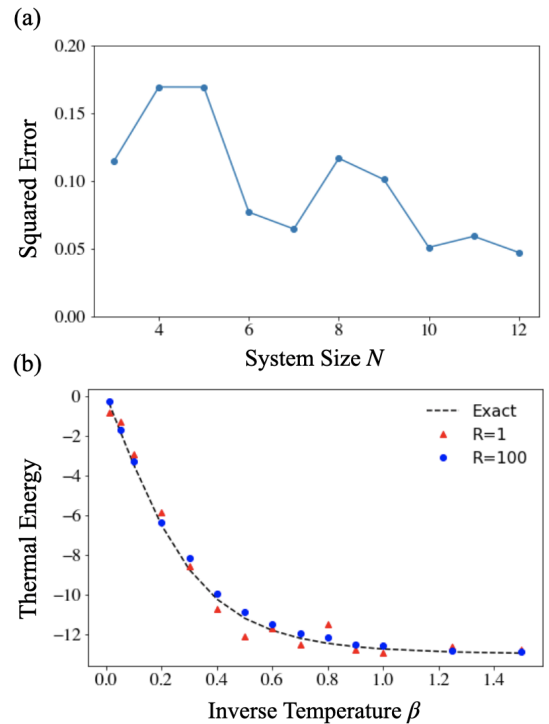


FIG. 2: (a) Squared error of thermal energy calculated from TPQ states with $d = 50$ as a function of system size N for a 1D Heisenberg model at inverse temperature $\beta = 0.5$. Results are averaged over 100 TPQ state realizations. (b) Comparing thermal energies of a 6-spin Heisenberg model as a function of inverse temperature β calculated from a single TPQ state and 100 TPQ states ($R=1$ and $R=100$ respectively). Exact values are shown for comparison.

In Fig. 3, we present numerical results demonstrating the efficacy of the algorithm in calculating thermal energies of 12-spin 1D and 2D Heisenberg models at various inverse temperatures. The random circuits are built through the aforementioned protocol and the non-unitary operation \hat{Q} is numerically simulated. The thermal energies in both the 1D and 2D systems are closely approximated by averaging over just 10 canonical TPQ states.

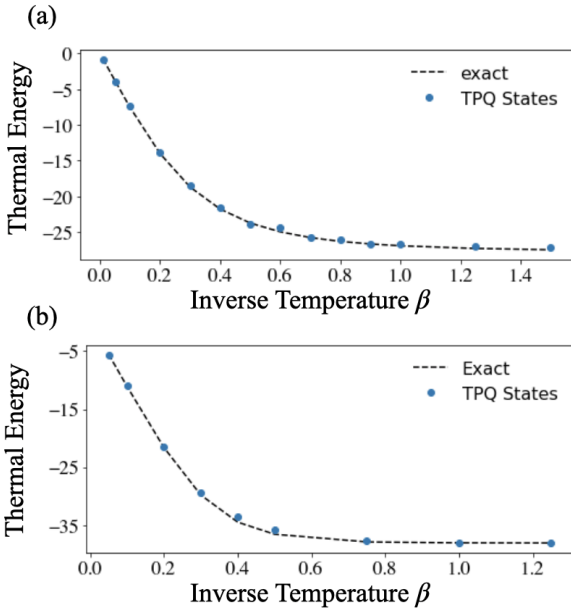


FIG. 3: Thermal energy, as a function of inverse temperature β of a (a) 1D Heisenberg model on a 12-qubit lattice (b) 2D Heisenberg on a 4x3 lattice. Shown are results averaged over 10 TPQ state realizations. The true ensemble thermal energy is shown by the dashed black line.

Next, we demonstrate quantum simulator results of our algorithm by using two different methods to approximate \hat{Q} with quantum circuits. In Fig. 4a, the thermal energy of a 3-qubit 1D Heisenberg model as a function of inverse temperature β is approximated using QITE to approximate \hat{Q} . The QITE circuit was generated using XACC [33]. Results are averaged over $R = 10$ TPQ states, with error bars showing one standard deviation. In Fig. 4b, the thermal energy of a 5-qubit 1D Heisenberg model as a function of inverse temperature is approximated using the dilated operator approach to implement \hat{Q} . Results using two different values of the dilated operator parameter ϵ are included to demonstrate its impact on performance. While smaller ϵ leads to significantly better results for larger β , it requires many more executions as the success probability decreases with smaller ϵ . After constructing the requisite dilated operator to approximate the non-unitary transformation \hat{Q} , Qiskit was utilized to decompose it into a circuit with the basis gate set of the IBM’s “ibmq_quito” device. Presented results are averaged over $R = 10$ distinct TPQ states, and the error bars

show one standard deviation.

Conclusion—We have presented a new method for approximating finite temperature properties of materials on quantum computers and demonstrated its efficacy through approximating thermal energies of Heisenberg models in one and two dimensions. To demonstrate flexibility in how the non-unitary step of the algorithm is performed, we presented quantum simulator results from performing the necessary non-unitary transforma-

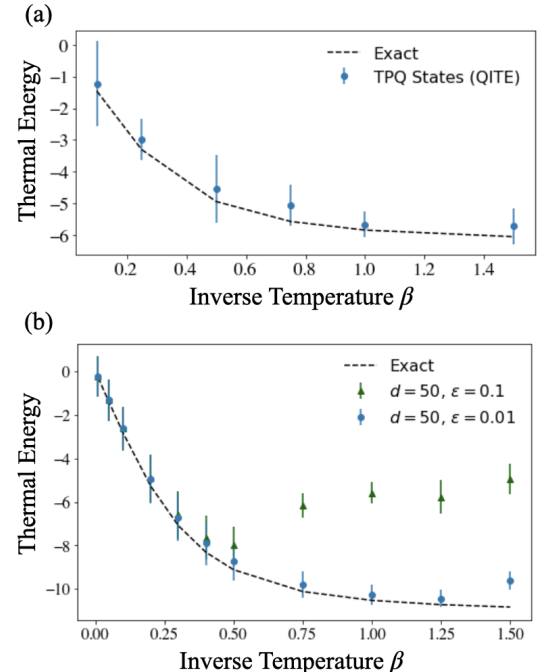


FIG. 4: Thermal energy, as a function of inverse temperature β of a (a) 3-qubit 1D Heisenberg model using the QITE algorithm to approximate \hat{Q} (b) 5-qubit 1D Heisenberg model using the dilated operator approach to approximate \hat{Q} .

tion with QITE and with a dilated operator approach. As the resources required by this algorithm scale inversely with system size, we expect it to be increasingly useful as we progress through the NISQ era and beyond.

Acknowledgments.—This research was supported by the Office of Science, Office of Advanced Scientific Computing Research Accelerated Research for Quantum Computing Program of the U.S. Department of Energy under Contract No. DE-AC02-05CH11231.

[1] D. Zhu, S. Johri, N. M. Linke, K. A. Landsman, C. Huerta Alderete, N. H. Nguyen, A. Y. Matsuura, T. H. Hsieh, and C. Monroe, Generation of thermofield double states and critical ground states with a quantum computer, *Proceedings of the*

National Academy of Sciences **117**, 25402 (2020), <https://www.pnas.org/content/117/41/25402.full.pdf>.
[2] G. Zhang and B. Li, Impacts of doping on thermal and thermoelectric properties of nanomaterials, *Nanoscale* **2**, 1058 (2010).

- [3] H. De Raedt, F. Jin, D. Willsch, M. Willsch, N. Yoshioka, N. Ito, S. Yuan, and K. Michielsen, Massively parallel quantum computer simulator, eleven years later, *Computer Physics Communications* **237**, 47 (2019).
- [4] S. Lloyd, Universal quantum simulators, *Science* **273**, 1073 (1996).
- [5] D. S. Abrams and S. Lloyd, Simulation of many-body Fermi systems on a universal quantum computer, *Phys. Rev. Lett.* **79**, 2586 (1997).
- [6] A. Smith, M. S. Kim, F. Pollmann, and J. Knolle, Simulating quantum many-body dynamics on a current digital quantum computer, *npj Quantum Information* **5**, 10.1038/s41534-019-0217-0 (2019).
- [7] L. Bassman, K. Liu, A. Krishnamoorthy, T. Linker, Y. Geng, D. Shebib, S. Fukushima, F. Shimojo, R. K. Kalia, A. Nakano, and et al., Towards simulation of the dynamics of materials on quantum computers, *Physical Review B* **101**, 10.1103/physrevb.101.184305 (2020).
- [8] L. Bassman, R. V. Beeumen, E. Younis, E. Smith, C. Iancu, and W. A. de Jong, Constant-depth circuits for dynamic simulations of materials on quantum computers (2021), arXiv:2103.07429 [quant-ph].
- [9] K. L. Brown, W. J. Munro, and V. M. Kendon, Using quantum computers for quantum simulation, *Entropy* **12**, 2268 (2010).
- [10] D. Poulin and P. Wocjan, Sampling from the thermal quantum gibbs state and evaluating partition functions with a quantum computer, *Phys. Rev. Lett.* **103**, 220502 (2009).
- [11] A. Riera, C. Gogolin, and J. Eisert, Thermalization in nature and on a quantum computer, *Physical Review Letters* **108**, 10.1103/physrevlett.108.080402 (2012).
- [12] E. Bilgin and S. Boixo, Preparing thermal states of quantum systems by dimension reduction, *Phys. Rev. Lett.* **105**, 170405 (2010).
- [13] J. Preskill, Quantum computing in the nisq era and beyond, *Quantum* **2**, 79 (2018).
- [14] G. Verdon, J. Marks, S. Nanda, S. Leichenauer, and J. Hidary, Quantum hamiltonian-based models and the variational quantum thermalizer algorithm (2019), arXiv:1910.02071 [quant-ph].
- [15] J. Wu and T. H. Hsieh, Variational thermal quantum simulation via thermofield double states, *Physical Review Letters* **123**, 10.1103/physrevlett.123.220502 (2019).
- [16] B. M. Terhal and D. P. DiVincenzo, Problem of equilibration and the computation of correlation functions on a quantum computer, *Phys. Rev. A* **61**, 022301 (2000).
- [17] A. N. Chowdhury and R. D. Somma, Quantum algorithms for gibbs sampling and hitting-time estimation, *Quantum Info. Comput.* **17**, 41–64 (2017).
- [18] M. Motta, C. Sun, A. T. K. Tan, M. J. O’Rourke, E. Ye, A. J. Minnich, F. G. S. L. Brandão, and G. K.-L. Chan, Determining eigenstates and thermal states on a quantum computer using quantum imaginary time evolution, *Nature Physics* **16**, 205–210 (2019).
- [19] S.-N. Sun, M. Motta, R. N. Tazhigulov, A. T. Tan, G. K.-L. Chan, and A. J. Minnich, Quantum computation of finite-temperature static and dynamical properties of spin systems using quantum imaginary time evolution, *PRX Quantum* **2**, 010317 (2021).
- [20] J. E. Moussa, Measurement-based quantum metropolis algorithm (2019), arXiv:1903.01451 [quant-ph].
- [21] K. Temme, T. J. Osborne, K. G. Vollbrecht, D. Poulin, and F. Verstraete, Quantum metropolis sampling, *Nature* **471**, 87–90 (2011).
- [22] M.-H. Yung and A. Aspuru-Guzik, A quantum-quantum metropolis algorithm, *Proceedings of the National Academy of Sciences* **109**, 754–759 (2012).
- [23] S. Lu, M. C. Bañuls, and J. I. Cirac, Algorithms for quantum simulation at finite energies, *PRX Quantum* **2**, 020321 (2021).
- [24] S. Sugiura and A. Shimizu, Canonical thermal pure quantum state, *Physical Review Letters* **111**, 10.1103/physrevlett.111.010401 (2013).
- [25] J. Richter and A. Pal, Simulating hydrodynamics on noisy intermediate-scale quantum devices with random circuits, *Physical Review Letters* **126**, 10.1103/physrevlett.126.230501 (2021).
- [26] R. M. Gingrich and C. P. Williams, Non-unitary probabilistic quantum computing, in *Proceedings of the Winter International Symposium on Information and Communication Technologies*, WISICT ’04 (Trinity College Dublin, 2004) p. 1–6.
- [27] O. V. Billoni, S. A. Cannas, and F. A. Tamarit, Spin-glass behavior in the random-anisotropy heisenberg model, *Physical Review B* **72**, 104407 (2005).
- [28] S.-S. Gong, W. Zhu, and D. Sheng, Emergent chiral spin liquid: Fractional quantum hall effect in a kagome heisenberg model, *Scientific reports* **4**, 1 (2014).
- [29] P. N. Jepsen, J. Amato-Grill, I. Dimitrova, W. W. Ho, E. Demler, and W. Ketterle, Spin transport in a tunable heisenberg model realized with ultracold atoms, *Nature* **588**, 403 (2020).
- [30] T. Tanaka and Y. Gohda, Prediction of the curie temperature considering the dependence of the phonon free energy on magnetic states, *npj Computational Materials* **6**, 1 (2020).
- [31] J. F. Rodriguez-Nieva, Turbulent relaxation after a quench in the heisenberg model, *Physical Review B* **104**, L060302 (2021).
- [32] Z.-W. Liu, *On Quantum Randomness and Quantum Resources*, Ph.D. thesis, Massachusetts Institute of Technology, Cambridge MA (2018).
- [33] A. J. McCaskey, D. I. Lyakh, E. F. Dumitrescu, S. S. Powers, and T. S. Humble, XACC: a system-level software infrastructure for heterogeneous quantum-classical computing, *Quantum Science and Technology* **5**, 024002 (2020).